ISSN 1064-2269, Journal of Communications Technology and Electronics, 2010, Vol. 55, No. 4, pp. 407–419. © Pleiades Publishing, Inc., 2010.
Original Russian Text © O.I. Moskalenko, A.A. Ovchinnikov, 2010, published in Radiotekhnika i Electronika, 2010, Vol. 55, No. 4, pp. 436–449.

DYNAMICS CHAOS IN RADIOPHYSICS AND ELECTRONICS

Investigation of the Noise Influence on Generalized Chaotic Synchronization in Dissipatively Coupled Dynamic Systems: Synchronous Regime Stability in the Presence of External Noise and Possible Practical Applications

O. I. Moskalenko and A. A. Ovchinnikov

Received August 14, 2009

Abstract—The noise influence on generalized synchronization in dissipatively coupled chaotic systems has been investigated. The threshold of the onset of the synchronous regime was shown to be scarcely dependent on the noise intensity. The reasons underlying the revealed feature have been analyzed via the modified system method and confirmed by numerical simulation data and experimental results. Practical applications of the revealed feature have been found. The method of hidden data transmission over communications channels with high noise levels is proposed.

DOI: 10.1134/S1064226910040066

INTRODUCTION

In the modern theory of nonlinear oscillations, synchronization of chaotic oscillations is one of the basic phenomena drawing scrupulous attention of researchers [1, 2]. Interest in this phenomenon is associated with both the fundamental significance of its research [1] and numerous practical applications, such as transmitting hidden information [3–9]; solving biological, chemical, and physical tasks [10–13]; and controlling chaotic motions, including chaotic oscillations in microwave electronic systems [14–17].

At present, researchers have revealed several types of the synchronous behavior of unidirectionally coupled dynamic systems, namely, phase synchronization (PS) [18], generalized synchronization (GS) [19], time-lagged synchronization [20], complete synchronization (CS) [21], noise-induced synchronization (NIS) [22], time-scale synchronization [23], etc., each of which has specific properties.

In the study of the GS phenomenon, one of the most important aspects is the influence of noise on transition to synchronous regimes [24–33]. It is known that noise can induce both constructive and destructive changes in the behavior of systems. In particular, under the action of noise on CS, the synchronous regime can be destroyed due to the local instability of synchronous manifold accompanied by the effect of on-off intermittency [34, 35]. However, common noise is capable of synchronizing two noninteracting but identical systems (starting with different initial conditions). In this case, the NIS regime is recognized [22, 25, 31, 36, 37]. The action of external noise on PS gives rise to a shift in the coupling parameter's threshold values corresponding to the onset of the synchronous regime [38]. Nevertheless, in the case of PS, noise can play a constructive role, enhancing the synchronous regime below the threshold of its origin [28].

In the recent literature, little attention has been paid to the noise influence on GS. An exception is paper [33] in which the authors examined the noise influence on GS in absolutely diverse unidirectionally coupled dynamic systems. It has been shown that noise plays a "system-dependent" role, i.e., can both enhance or induce and, on the contrary, destroy the GS regime.

In this paper, for the first time, the noise influence on transition to GS between dissipatively coupled chaotic systems (with slightly mismatched parameters) is investigated theoretically and confirmed by the results of experiments. Below, it is shown that noise hardly affects the threshold of the onset of the GS regime in such systems. Therefore, the GS regime is resistant to the action of noise. The discovered feature can find applications in different fields of science and technology, e.g., for hidden data transmission over communications channels at sufficiently high levels of noise [39, 40].

1. REGIME OF THE GENERALIZED SYNCHRONIZATION BETWEEN CHAOTIC OSCILLATORS

Generalized synchronization is introduced into consideration for unidirectionally coupled driving ($\vec{\mathbf{x}}(t)$) and response ($\vec{\mathbf{u}}(t)$,) chaotic oscillators and implies that the functional relation $\vec{\mathbf{u}}(t) = \vec{\mathbf{F}}[\vec{\mathbf{x}}(t)]$ [19]

appears between their states after a transient process finished. Its form $\vec{\mathbf{F}}[\cdot]$ can be fairly intricate and require a nontrivial procedure of determination [41].

In the literature, several techniques has been proposed to diagnose the GS regime: the method of nearest neighbors [19, 42], the calculation of conditional Lyapunov exponents (CLEs) [43, 44], and the auxiliary system approach [45], which finds frequent use and can easily be implemented.

The auxiliary system method relies on constructing and considering auxiliary system $\vec{\mathbf{v}}(t)$ identical to response system $\vec{\mathbf{u}}(t)$. It is assumed that the initial conditions of the auxiliary system, $\vec{\mathbf{v}}(t_0)$, differ from the initial state of the response system, $\vec{\mathbf{u}}(t_0)$,, but belong to the basin of attraction of the same attractor. In the absence of the GS regime between the interacting systems, the state vectors of response and auxiliary systems ($\vec{\mathbf{u}}(t)$ and $\vec{\mathbf{v}}(t)$, respectively) share the same chaotic attractor but are different. After the onset of the GS regime, the states of response and auxiliary systems must be identical, namely,

$$\vec{\mathbf{u}}(t) = \vec{\mathbf{F}}[\vec{\mathbf{x}}(t)],$$

because the relationships

$$\vec{\mathbf{v}}(t) = \vec{\mathbf{F}}[\vec{\mathbf{x}}(t)],$$

and, therefore,

$$\vec{\mathbf{u}}(t) \equiv \vec{\mathbf{v}}(t),$$

become valid after a transient process finished. The identity of states is the criterion indicating the presence of GS between driving and response oscillators.

The GS regime can also be analyzed by calculating the CLEs [43, 44]. If driving and response systems have phase spaces with respective dimensions N_d and N_r,, the behavior of unidirectionally coupled oscillators can be characterized by the spectrum of Lyapunov exponents $\lambda_1 \geq \lambda_2 \geq \ldots \geq \lambda_{N_d+N_r}$. Since the driving system behavior does not depend on the state of the response oscillator, the spectrum of Lyapunov exponents can be divided into the driving system's Lyapunov exponents

$$\lambda_1^d \geq \ldots \geq \lambda_{N_d}^d,$$

and the CLEs

$$\lambda_1^r \geq \ldots \geq \lambda_{N_r}^r.$$

The criterion that GS exists in unidirectionally coupled systems [41, 43] is the presence of negative largest CLE λ_1^r..

It is known that the GS regime can be observed in systems with dissipative and nondissipative couplings [41, 46]. For dissipatively coupled systems discussed below, the equations describing the dynamics of interacting systems can be written [46] as

$$\begin{aligned} \dot{\vec{\mathbf{x}}}(t) &= \mathbf{G}(\vec{\mathbf{x}}(t), \vec{\mathbf{g}}_d), \\ \dot{\vec{\mathbf{u}}}(t) &= \mathbf{H}(\vec{\mathbf{u}}(t), \vec{\mathbf{g}}_r) + \varepsilon \mathbf{A}(\vec{\mathbf{x}}(t) - \vec{\mathbf{u}}(t)), \end{aligned} \tag{1}$$

Here, $\vec{\mathbf{x}}(t)$ and $\vec{\mathbf{u}}(t)$ are the state vectors of driving and response systems, respectively; $\mathbf{G}$ and $\mathbf{H}$ determine the vector fields of interacting systems; $\vec{\mathbf{g}}_d$ and $\vec{\mathbf{g}}_r$ are the vectors of control parameters; $\mathbf{A} = \{\delta_{ij}\}$ is the coupling matrix; $\delta_{ii} = 0$ or 1 and $\delta_{ii} = 1$, $\delta_{ij} = 0$ ($i \neq j$), ε is the coupling parameter.

The mechanisms by which the GS regime arises can be revealed via the modified system method proposed in our papers [46, 47]. According to this approach, response system $\vec{\mathbf{u}}(t)$ is assumed to be the modified system

$$\dot{\vec{\mathbf{u}}}_m(t) = \mathbf{H}'(\vec{\mathbf{u}}_m(t), \vec{\mathbf{g}}_r, \varepsilon), \tag{2}$$

under external action $\varepsilon(\mathbf{A}\vec{\mathbf{x}}(t) + D\xi(t))$,

$$\dot{\vec{\mathbf{u}}}_m(t) = \mathbf{H}'(\vec{\mathbf{u}}_m(t), \mathbf{g}_r, \varepsilon) + \varepsilon(\mathbf{A}\vec{\mathbf{x}}(t) + D\xi(t)), \tag{3}$$

Here, $\mathbf{H}'(\vec{\mathbf{u}}(t)) = \mathbf{H}(\vec{\mathbf{u}}(t)) - \varepsilon\mathbf{A}\vec{\mathbf{u}}(t)$. where term $-\varepsilon\mathbf{A}\vec{\mathbf{u}}(t)$ brings the additional dissipation into modified system (2).

It can be assumed that the GS regime arising in system (1) is a consequence of two simultaneous mutually coupled processes in which both the dissipation in modified system (2) and the amplitude of an external signal increase [46, 47]. The increased dissipation in modified system (2) simplifies its behavior and causes the transition from chaotic to periodic oscillations occurs (i.e., a stationary state is implemented). The external action, on the contrary, tends to complicate the behavior of the modified system and imposes its own dynamics. It has been shown [46, 47] that the transition to the GS regime becomes possible only when the own chaotic dynamics of the response system is suppressed by dissipation.

Thus, the GS stability is determined mainly by the properties of the modified system. When added to the equations of system (1), external noise $\mathbf{B}D\xi(t)$ ($\mathbf{B}$ is the coupling matrix similar to $\mathbf{A}$) must only lead to a negligible change in the characteristics of the modified system. Since the characteristics of modified system (2) very slightly depend on the additive noise, its influence on the threshold of the onset of the GS regime in (1) must not be very strong.

Indeed, as mentioned above, the GS regime can be analyzed by calculating the CLEs. It is evident that the response and auxiliary systems can be regarded as two identical systems starting with close initial conditions. Let us calculate the derivative of the difference between their states,

$$\vec{\Delta}(t) = \vec{\mathbf{v}}(t) - \vec{\mathbf{u}}(t),$$

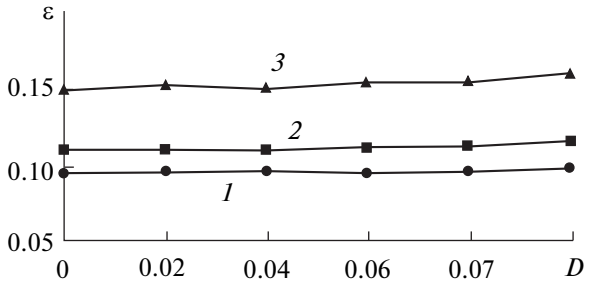

Fig. 1. Dependences between the threshold of the onset of the GCS regime in two unidirectionally coupled logistic maps and the noise intensity for the following values of control parameters: $\lambda_x = 3.75$, $\lambda_y = 3.75$ (*1*), $\lambda_x = 3.75$, $\lambda_y = 3.79$ (*2*), $\lambda_x = 3.75$, $\lambda_y = 3.9$ (*3*).

in the presence ($D > 0$) and absence ($D = 0$) of noise. Since each of two systems is excited by identical deterministic and stochastic signals, we obtain the same equation

$$\dot{\Delta}(t) = (\mathbf{J}\mathbf{H}(\vec{\mathbf{u}}(t)) - \varepsilon\mathbf{A})\vec{\Delta}(t) = \mathbf{J}\mathbf{H}'(\vec{\mathbf{u}}(t))\vec{\Delta}(t), \quad (4)$$

where **J** is the Jacobian matrix. In the calculation of the CLEs, Eq. (4) can be regarded as the variational equation. Hence, it can be inferred that largest CLEs λ_1^r, (their values determine the threshold of the onset of the GS regime) will behave alike when noise is both present and absent, intersecting the threshold $\lambda_1^r = 0$ at the same values of ε, corresponding to the onset of the GS regime. Therefore, according to Eq. (4), the threshold value of the coupling parameter must be independent of the noise intensity, and the type synchronous behavior must be highly resistant to noise. It should be emphasized that the response system's state vector $\vec{\mathbf{u}}(t)$ in (4) depends on random signal ξ,. Therefore, noise with high intensity D can change the properties of the modified system and, finally, can change the boundary of the onset of the GS regime.

2. NOISE INFLUENCE ON THE ONSET OF THE GENERALIZED SYNCHRONIZATION REGIME IN MODEL SYSTEMS: NUMERICAL SIMULATION

To confirm the validity of theoretical foundations presented in Section 1, we consider the known dynamic systems capable of demonstrating the generalized synchronization regime under the action of additional external noise and numerically simulate their behavior. As examples of dynamic systems, discrete-time systems (unidirectionally coupled logistic maps) and chaotic oscillators (unidirectionally coupled Rössler systems) are investigated.

A. Logistic Maps

As the first example, let us consider the behavior of unidirectionally coupled logistic maps [44] in the case where an external noise source is additionally affects the response system:

$$\begin{aligned} x_{n+1} &= f(x_n, \lambda_x), \\ y_{n+1} &= f(y_n, \lambda_y) + \varepsilon(f(x_n, \lambda_x) + Df(\xi, \lambda_x) - f(y_n, \lambda_y)), \end{aligned} \quad (5)$$

Here, $f(x,\lambda) = \lambda x(1 - x)$, $\lambda_{x,y}$ are the control parameters of driving and response systems, respectively; quantity ε characterizes the intensity of coupling between oscillators; ξ is the random process whose probability density is uniformly distributed over the unit interval [0; 1]; and D is the noise intensity. To diagnose the GS regime in system (5) under study, the auxiliary system method was used.

Figure 1 illustrates the dependences between the threshold of the onset of the GS regime and the noise intensity. The threshold curves are constructed on the "noise intensity D–coupling parameter ε" plane for different values of control parameters $\lambda_{x,y}$. It is evident that the threshold value of the coupling parameter hardly depends on the noise intensity $D \in [0; 0.1]$ at all. To explain such behavior of the systems under investigation, it is necessary to consider the modified system

$$z_{n+1} = (1 - \varepsilon)f(z_n, \lambda_y) = az_n(1 - z_n), \quad (6)$$

where $a = \lambda_y(1 - \varepsilon)$. Figure 2a depicts the bifurcation diagram that characterizes the behavior of the modified system depending on parameter ε, It is seen that modified system (6) begins demonstrating periodic oscillations when the coupling parameter reaches its threshold value corresponding to the onset of the GS regime in system (5). The external noise action hardly changes the characteristics of the modified system and, therefore, hardly affects the threshold of the onset of GS. Figure 2b depicts the bifurcation diagram of the modified system obtained in the presence of

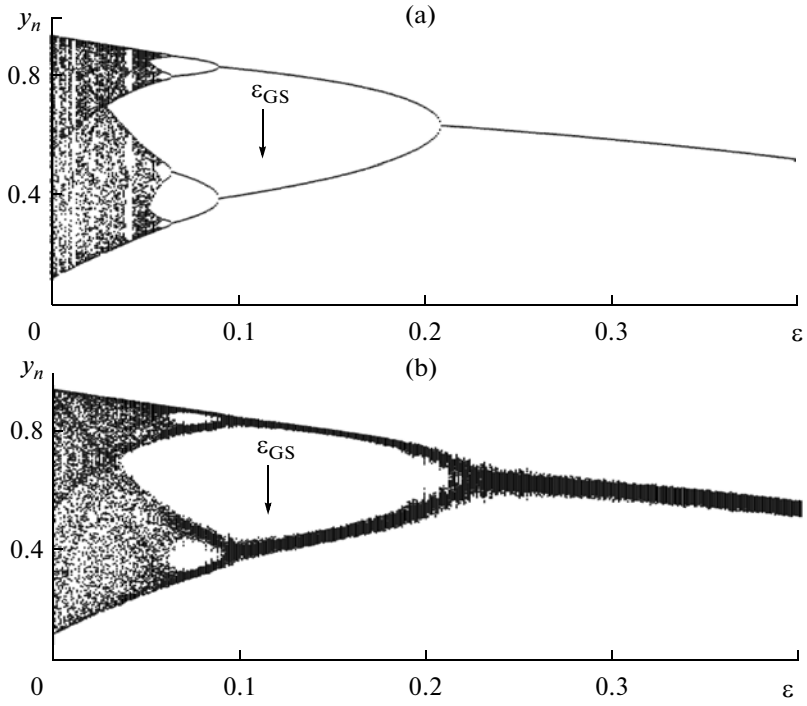

Fig. 2. Bifurcation diagrams of modified logistic map (6) in the (a) absence and (b) presence of noise. The control parameter is (a, b) $\lambda_y = 3.79$; the noise intensity is (b) $D = 0.1$. The arrows indicate the threshold values of coupling parameter corresponding to the threshold of the onset of the GS regime(ε_{GS}).

noise with the intensity $D = 0.1$. The shape of the bifurcation diagram indicates that the noise level is substantially higher than the signal amplitude. At the same time, it is obvious that, in this case, the external noise gives rise to the noisy regime implemented in the system rather than to the shift of the bifurcation point. Hence, it can be inferred that an external noise scarcely affects the onset of the GS regime in discrete-time systems although its amplitude is fairly high.

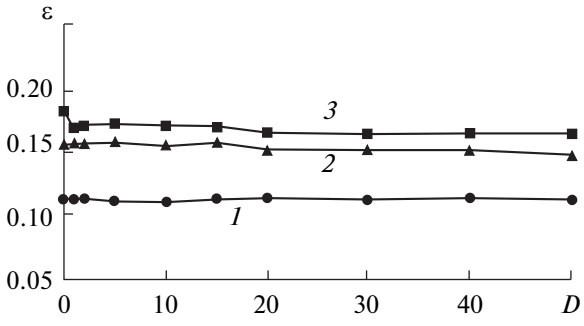

Fig. 3. Dependences between the threshold of the onset of the GCS regime in two unidirectionally coupled Rössler oscillators (7) and the noise intensity for the driving system's parameter (*1*) $\omega_x = 0.99$, (*2*) 0.95, and (*3*) 0.91.

B. Rössler Systems

As the second example, let us consider two unidirectionally coupled Rössler systems

$$\begin{aligned}\dot{x}_1 &= -\omega_x x_2 - x_3 + D_1\xi,\\ \dot{x}_2 &= \omega_x x_1 + a x_2,\\ \dot{x}_3 &= p + x_3(x_1 - c),\end{aligned}$$

$$\begin{aligned}\dot{u}_1 &= -\omega_u u_2 - u_3 + \varepsilon(x_1 + D_2\zeta - u_1),\\ \dot{u}_2 &= \omega_u u_1 + a u_2,\\ \dot{u}_3 &= p + u_3(u_1 - c),\end{aligned} \qquad (7)$$

where

$$\vec{\mathbf{x}}(t) = (x_1, x_2, x_3)^T \text{ and } \vec{\mathbf{u}}(t) = (u_1, u_2, u_3)^T$$

are the state vectors of driving and response systems, respectively, and $a = 0.15$, $p = 0.2$, $c = 10$, ω_x, and $\omega_u = 0.95$ are the control parameters. In the above equations, parameters $\omega_{x,u}$ determine the oscillation eigenfrequencies in driving and response systems; summands $D_1\xi$, $D_2\zeta$ assign an external action on the interacting systems; and ξ, ζ are Gaussian random processes with zero means and unit variances. Equations (7) were integrated via the fourth-order Runge–Kutta method adapted to the stochastic differential

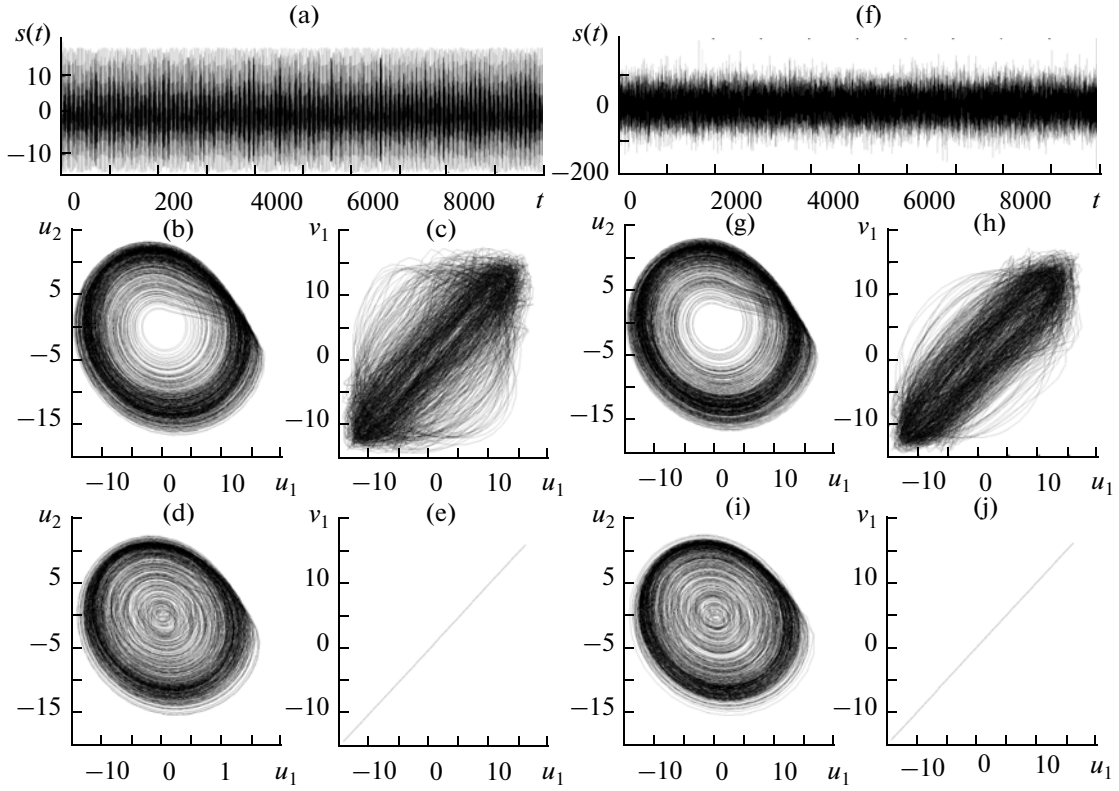

Fig. 4. (a, f) Signals $s(t)$, affecting the response and auxiliary systems. (b, d, g, i) Phase portraits of the response system and (c, e, h, j)(u_1, v_1), planes characterizing the behavior of the response and auxiliary systems ($\varepsilon = 0.05$) below and ($\varepsilon = 0.114$) above the boundary of transition to GS in the unidirectionally coupled Rössler systems for $\omega_d = 0.99$. The presented signals, phase portraits and $((u_1, v_1),)$ planes correspond to (a–e) the absence of noise ($D = 0$) and (f–j) the presence of noise with the intensity $D = 40$.

equations [48]. The time step was $\Delta t = 0.001$. The diagnostics of the generalized chaotic synchronization (GCS) regime was implemented via the auxiliary system method (see Section 1).

Let a noise signal only affect the response system; i.e., $D_1 = 0$, $D_2 = D$. Figure 3 illustrates the dependences between the threshold of the onset of the GCS regime and the noise intensity. The threshold curves were obtained for three different values of control parameter ω_x and the fixed values of other parameters. To obtain a comprehensive picture of the onset of GS, the control parameters were selected to be $\omega_x = 0.99$ (a comparatively large frequency mismatch between the interacting chaotic oscillators), $\omega_x = 0.95$ (identical oscillators), and $\omega_x = 0.91$ (small frequency mismatches). It is clear that the boundary of transition to the GCS regime is hardly dependent on the noise intensity D at all values of control parameter ω_x. Even when its values are large enough ($D > 20$), the GS regime arises at the values of coupling parameter ε that are approximately the same as in the absence of noise.

Figure 4 depicts the signals $s(t) = x_1(t) + D\xi(t)$ acting on the response and auxiliary systems in the absence and presence of noise as well as the phase portraits of the response system and planes $((u_1, v_1),)$ characterizing the behavior of the response and auxiliary systems before and after the onset of the GS regime. Figures 4a–4e and 4f–4j refer, respectively, to the scenarios without noise and with noise affecting the response system. In the latter scenario, the noise intensity is $D = 40$, and the external action is similar

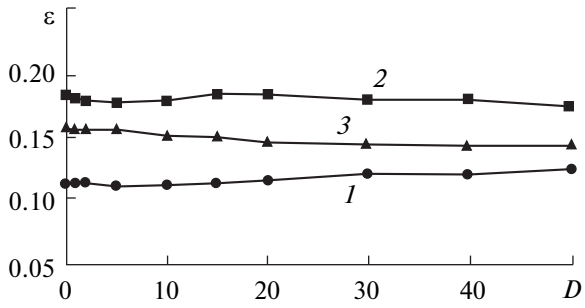

Fig. 5. Dependences between the threshold of the onset of the GCS regime in two unidirectionally coupled Rössler oscillators (7) and the noise intensity. The threshold curves were obtained under the action of a common noise source for the driving system's parameter (*1*) $\omega_x = 0.99$, (*2*) 0.95, and (*3*) 0.91.

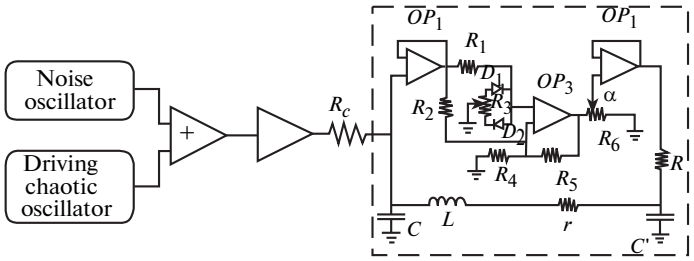

Fig. 6. Block diagram of the experimental setup used to examine the noise influence on the stability of the GCS regime. The schematic diagram of the chaotic oscillator is shown within the dotted rectangle and involves the following components: $C = 300$ nF, $C' = 150$ nF, $R = 630\ \Omega$, $r = 56\ \Omega$, $L = 3.3$ mH, $OP_{1,2}$ (TL082 operational amplifiers), OP_3 (LF356N operational amplifier), $D_{1,2}$ (1N4118 diodes), $R_1 = 2.7$ kΩ, $R_2 = R_4 = 7.4$ kΩ, $R_3 = 100\ \Omega$, $R_5 = 186$ kΩ, $R_6 = 4.7$ kΩ, and RC'. The parameter characterizing a nonlinear converter and a coupling resistor are designated with α and R_c, respectively.

to a stochastic signal (compare Figs. 4a and 4f). It is seen from these figures that the response system characteristics remain practically unchanged with increasing noise intensity (compare Figs. 4b, 4d and 4g, 4i). Therefore, it can be said that, for unidirectionally coupled Rössler systems, the modified system

$$\begin{aligned} \dot{z}_1 &= -\omega_u z_2 - z_3 - \varepsilon z_1, \\ \dot{z}_2 &= \omega_u z_1 + a z_2, \\ \dot{z}_3 &= p + z_3(z_1 - c), \end{aligned} \tag{8}$$

where $\vec{\mathbf{z}} = (z_1, z_2, z_3)^T$ is the state vector, demonstrates the invariability of stability properties under the action of high-intensity noise. Thus, when the control parameters are selected as mentioned above, a stable cycle of period 1 is implemented in modified system (8) (see also [47]).

It is significant that the coupling parameter's threshold value corresponding to the onset of the GCS regime is the weakly dependent on the noise intensity if an additional noise source also affects the first oscillator (i.e., $D_1 \neq 0$). The value of this parameter was selected to be $D_1 = \varepsilon D$.. Figure 5 illustrates the dependences between the coupling parameter's threshold value and the noise intensity under the action of a common noise source. In this case, the behavior of the interacting systems is entirely determined by the mechanisms described above.

Thus, in the cases discussed above, the threshold of the onset of the GCS regime was confirmed to be almost completely independent of the noise intensity. Therefore, it is possible to infer the stable behavior of GCS arising in the systems with a small number of degrees of freedom under the action of external noise.

3. EXPERIMENTAL INVESTIGATION OF THE NOISE INFLUENCE ON THE THRESHOLD OF THE ONSET OF THE GENERALIZED CHAOTIC SYNCHRONIZATION REGIME

To confirm the results of theoretical prediction and numerical simulation data from the previous sections, the noise influence on the stability of generalized synchronization has been investigated experimentally. The objects of experiments were simple radiotechnical oscillators, which were capable of demonstrating the chaotic dynamics and had easily controlled parameters (including the intensity of external actions).

The block diagram of the experimental setup is depicted in Fig. 6. As the base element of the setup, a radiotechnical oscillator (similar to the oscillator described in [49, 50]) with a nonlinear component and a feedback loop was used. Depending on the selected parameters, this oscillator can excite both periodic and chaotic oscillations. Hence, the value of parameter α was selected so as to ensure its operation in the regime of chaotic oscillations. The chaotic oscillator was connected to an L-Card L783 data acquisition module, which was built into a personal computer and used to record variations in voltages across capacitors C and C'. The obtained time series were analyzed numerically.

An analog driving signal was formed by a digital-to-analog converter (DAC) from the signal of the aforementioned oscillator, which was previously digitized and recorded by means of an analog-to-digital converter (ADC). This signal was introduced into the system through the unidirectional dissipative coupling (see Fig. 6). A noise signal was formed with the help of an Agilent 33220 function generator and introduced through a summator into a communication device. The noise signal was a δ-correlated white noise with the Gaussian distribution of amplitudes. Oscillations

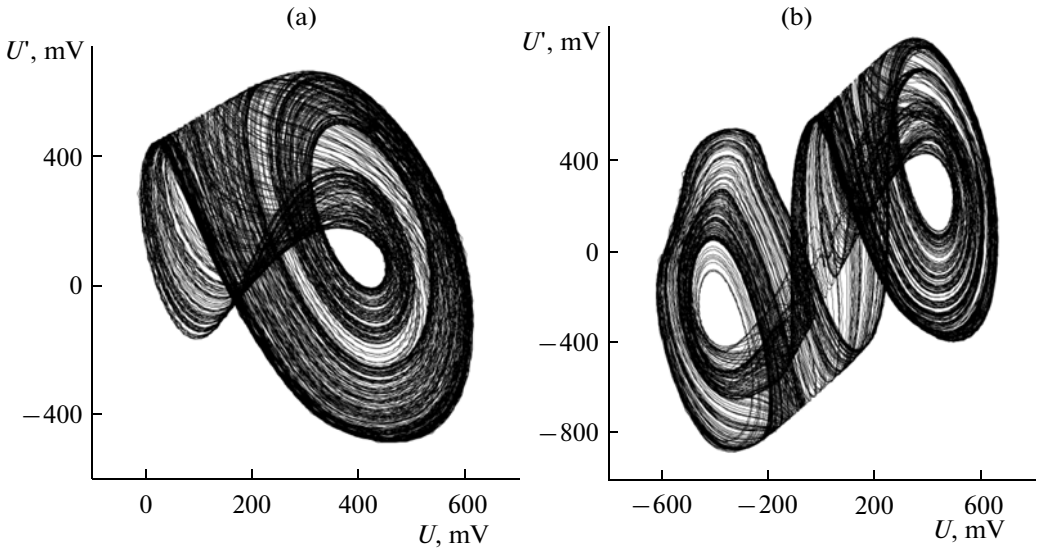

Fig. 7. Typical phase portraits of chaotic oscillations observed in the radiotechnical experiment with an autonomous oscillator: (a) belt-type attractor ($\alpha \approx 0.15$) and (b) double-scroll attractor ($\alpha \approx 0.25$).

of a response system were digitized and transmitted to a computer that performed their processing.

As noted above, the auxiliary system method ensures the most simple and efficient detection of the GCS regime. In this method, a response system is analyzed simultaneously with its precise copy (an auxiliary system) starting with distinct initial conditions. However, the obtainment of the precise copy of a radiotechnical oscillator is fairly complicated and nontrivial problem. The main impediment is the parameter spread inherent to each family of electronic devices. Such a problem is traditionally solved by selecting electronic devices with maximally similar parameters. However, this approach makes it possible to obtain a system whose parameters are approximately identical to those of the initial system, rather than its precise copy.

At the same time, in experimental investigation, the following approach is often employed (see, e.g., [51]). Two digitized signals of a driving system are transmitted to a response system, and the latter is regarded as a response oscillator for the first signal and as an auxiliary oscillator for the second signal. As a result, a distinction of initial conditions is implemented automatically.

After digitization, the mentioned time realizations without excluded initial fragments corresponding to a transient process are compared. In accordance with the basic idea of the auxiliary system method, the coincidence between these time realizations confirms the existence of the GCS regime.

The radiotechnical oscillator under investigation can demonstrate two typical regimes of chaos generation in which belt-type and double-scroll attractors are observed. Figure 7 depicts the typical phase portraits of oscillations corresponding to these regimes of an autonomous oscillator.

Three distinct cases of chaos behavior were implemented during experimental investigations:

(i) Chaotic oscillations excited in the autonomous driving and response oscillators are characterized by belt-type attractors.

(ii) The chaotic regime with a belt-type attractor is implemented in the driving oscillator, while a double-scroll attractor is observed in the response oscillator.

(iii) Chaotic oscillations of the autonomous driving and response oscillators are characterized by double-scroll chaotic attractors.

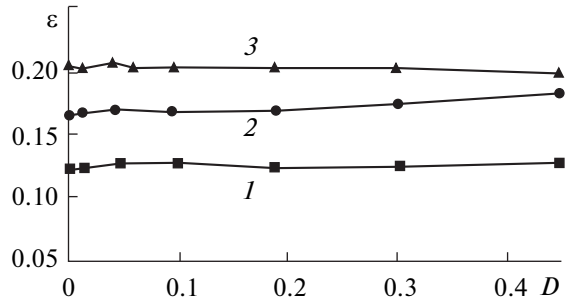

Fig. 8. Dependences between the coupling parameter corresponding to the onset of the GCS regime and the noise intensity: (curve *1*) two autonomous oscillators under consideration are characterized by belt-type attractors, (curve *2*) the driving system is characterized by a belt-type chaotic attractor; the response oscillator demonstrates chaotic oscillations associated with a double-scroll attractor, and (curve *3*) the autonomous driving and response oscillators are characterized by double-scroll chaotic attractors.

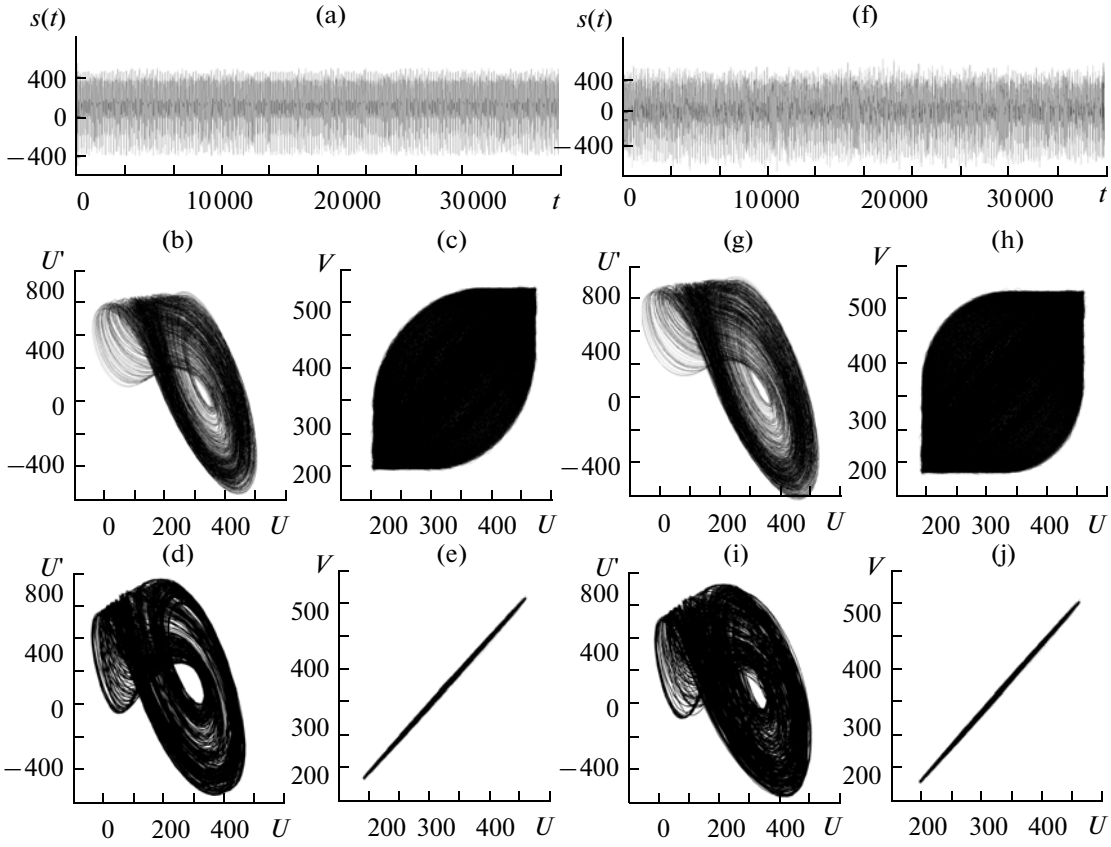

Fig. 9. Driving chaotic oscillator signals affecting the response oscillator in the (a) absence and (f) presence of a noise source. (b, d, g, i) Phase portraits of the response system and (c, e, h, j) (U,V) planes characterizing the behavior of the response and auxiliary systems ($\varepsilon = 0.22$) before and ($\varepsilon = 0.34$) after the onset of the GS regime. The control parameters of radiotechnical oscillators were selected so as to implement belt-type chaotic oscillations in two autonomous systems. The presented signals, phase portraits and (u_1, v_1) planes correspond to (a–e) the absence of noise ($D = 0$) and (f–j) the presence of noise with the intensity $D = 0.4$.

In each of the cases, different noise intensities were taken into consideration. For experimental data, the ratio of noise power P_n to chaotic signal power P_{cs}, $D = P_n/P_{cs}$, played the role of noise intensity.

Figure 8 illustrates the dependences between the threshold value of the coupling parameter

$$\varepsilon = 1/R_c\sqrt{L/C},$$

corresponding to the GCS regime and the noise intensity for three cases discussed above.

Figure 9 depicts the driving system signals acting on the response system in the absence and presence of an additive noise as well as the phase portraits of the response system and (U,V), planes characterizing the behavior of the response and auxiliary systems when the GS regime is absent and present in the radiotechnical oscillators with belt-type attractors. It is seen that the response system characteristics are scarcely changed under the action of noise. The similar situation is observed in the system involving two unidirectionally coupled radiotechnical oscillators both (or each) of which, if autonomous, have double-scroll attractors. Thus, it can be said that the modified system, i.e., an oscillator with additional dissipation, demonstrates periodic oscillations of period 1. A subsequent increase in the noise intensity (up to the values exceeding the deterministic signal intensity) can increase gradually the coupling parameter at which the GCS regime is stabilized.

Thus, experimental results agree well with both theoretical and numerical data discussed above and confirm the stability of the GCS regime under the action of noise.

4. PRACTICAL APPLICATIONS OF THE STABILITY OF THE GENERALIZED SYNCHRONIZATION REGIMEUNDER THE ACTION OF NOISE

The stability of the generalized synchronization regime under the action of external noise, which was revealed in Sections 2 and 3, can find applications, e.g., for hidden data transmission over communications channels with a high noise level. In addition, this feature can be employed to improve the data transmission confidentiality. In this case, a complex signal, a

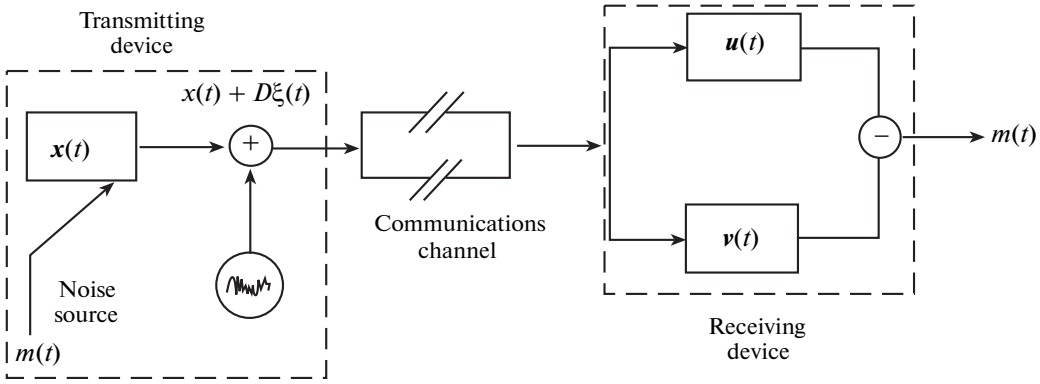

Fig. 10. Schematic diagram for implementing the hidden data transmission method based on the GCS regime in the presence of noise.

sum of a deterministic signal with useful information and a stochastic signal, is created and transmitted over a communication channel.

With the revealed feature taken into account, we propose a new hidden data transmission method based on GS in the presence of noise. Figure 10 depicts the schematic diagram of its implementation. The hidden data transmission method is intended for transmission of digital signals and is implemented as follows. Information signal $m(t)$ is represented as a binary code to modulate one or several control parameters of transmitting chaotic oscillator $\bar{\mathbf{x}}(t)$. In parameter modulation, transmitted signal characteristics must undergo insignificant changes and it is necessary to ensure the possibility of the onset or breakdown of the GS regime between the oscillators of transmitting and receiving devices, depending on the transmitted binary digit. For this purpose, the location of the GS boundary on the "modulation parameter–coupling strength" must have a distinctive feature consisting in that an insignificant change in the corresponding parameter must lead to an abrupt change in the threshold value of the onset of the synchronous regime. To ensure additional masking of an information signal and a change in the characteristics of a transmitted signal, a noise source is used. The signal generated in the transmitting system is mixed with a noise signal in the summator and is transmitted over a communications channel in which its characteristics are distorted under the action of noised inherent to al real devices. The receiving device is situated at the other end of the communications channel and involves two identical chaotic oscillators $\bar{\mathbf{u}}(t)$ and $\bar{\mathbf{v}}(t)$, operating in the GS regime with the transmitting oscillator. The principle of operation of the receiving device is based on the diagnostics of the GS regime via the auxiliary system method. The signal transmitted over the communications channel arrives at the inputs of two identical oscillators of the receiving device. Output signals pass through a subtractor. Thereafter, recovered information signal $\tilde{m}(t)$ is detected.

To verify the efficiency of the proposed hidden data transmission method, let us perform numerical simulation for the schematic diagram shown in Fig. 10. The oscillators of the transmitter and receiver are assumed to be unidirectionally coupled Rössler systems discussed in Section 2B, which have the same values of control parameters a, p, c, ω_u and the same distribution of random quantity ζ., The coupling parameter and the noise signal amplitude affecting the driving system are taken to be $\varepsilon = 0.14$, and $D_1 = 0$, respectively. The total noise intensity at the output of the noise source and in the communication channel is taken to be $D_2 = D = 10$. The control parameter ω_x of the transmitter's oscillator is modulated by a binary digital signal in the following way. If binary digit 1 is transmitted in the specified time interval, $\omega_x = 0.91$ within this interval. In the transmission of binary digit 0, parameter ω_x is a random value from the range of $\omega_x \in [0.9, 0.91)$; i.e., the parameter mismatch is extremely small (on the order of 1.1%).

The following reasons motivated us to select Rössler systems as the model oscillators of the transmitter and receiver:

(i) The synchronous behavior of Rössler systems, including GS [47, 52–54], have been investigated sufficiently well.

(ii) The location of the GS boundary satisfies the conditions mentioned above (see also [54]).

(iii) It is possible to construct a radiotechnical oscillator whose dynamics will be described by the Rössler system's equations [55].

The values of control parameters were selected on the basis of the character of location of the GS boundary. Note that parameter ω_x can take an arbitrary value, and the necessary condition is the interchange between regions with asynchronous dynamics and GS.

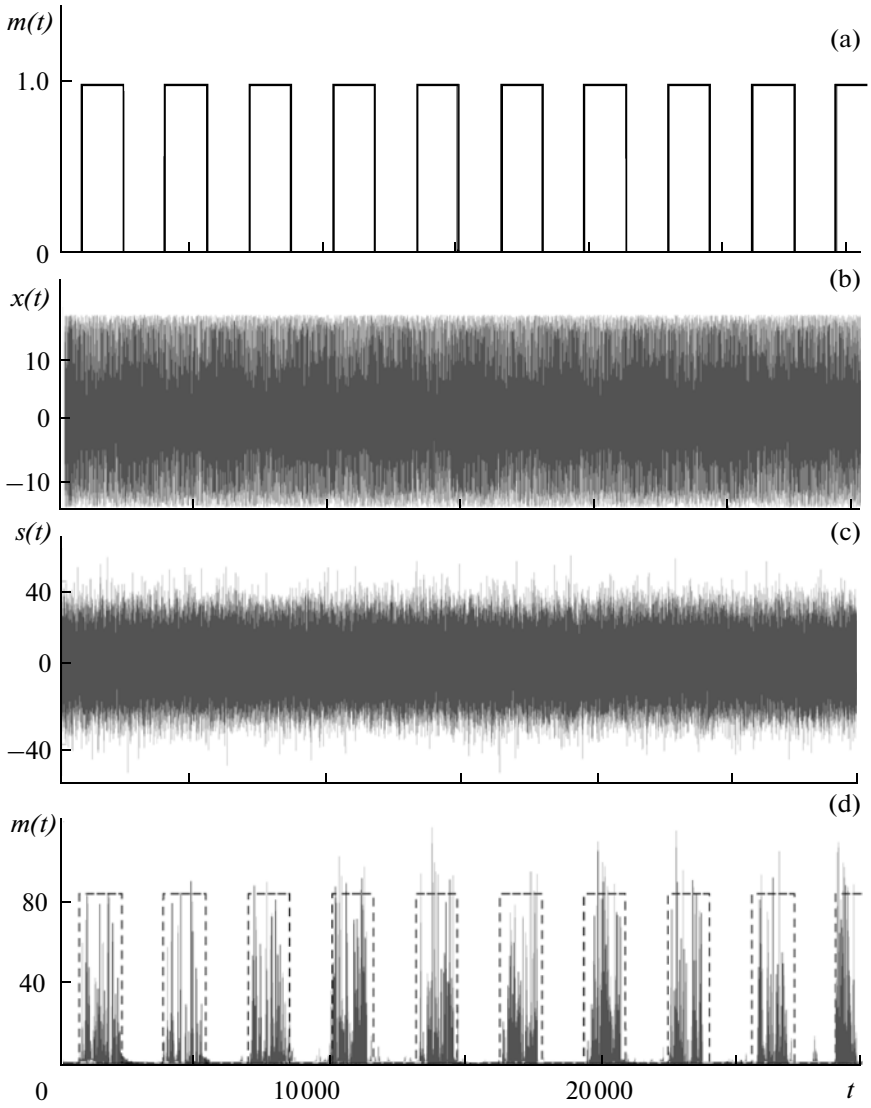

Fig. 11. An example of the numerical realization of the hidden data transmission method based on GCS in the presence of noise ($D = 10$): (a) information signal $m(t)$, represented as a simple sequence of binary digits 0 and 1; (b) signal $x(t)$, generated by the transmitting chaotic system, (c) signal $s(t)$, transmitted over the communications channel, and (d) (solid line) recovered signal $\tilde{m}(t)$ and (dashed line) the detected information signal at the output of a low-pass filter.

Figure 11 illustrate the efficiency of the proposed hidden data transmission method. For illustrative purposes, a simple sequence of binary digits 0 and 1 (Fig. 11a) is selected as information signal $m(t)$. As seen in Fig. 11b, the modulation of control parameter ω_x scarcely changes the characteristics of a signal produced by the transmitting chaotic oscillator. In addition, noise of sufficiently large intensity enhances distortions of the transmitted signal (Fig. 11c). In this case, unauthorized users cannot decode an initial data message without complete information about the characteristics of the receiving chaotic oscillator. At the same time, the quality of data recovered by the receiving device is high enough. It is not difficult to see that initial (Fig. 11a) and detected (the dashed line in Fig. 11d) information signals are identical. This confirms the high quality of data transmission. A similar situation is observed with an increase in noise intensity D. The proposed method becomes inefficient only when the ratio of the energy per bit to the noise power spectral density [56, 57] is $E_b/N_0 = -10.01$ dB.

The proposed hidden data transmission method was compared quantitatively with known analogues. For this purpose, the E_b/N_0 ratios at which the known hidden data transmission schemes based on chaotic synchronization [5, 58–63] remain efficient have been calculated. In calculations, unidirectionally coupled Rössler systems with the close values of control parameters were selected as the oscillators of transmitting and receiving devices. The calculated results are

Results of calculation

Scheme number	Scheme name	Reference	E_b/N_0, dB
1	Chaotic masking	[6]	56.48
2	Chaotic switching	[58]	30.76
3	Nonlinear mixing	[59]	64.99
4	Control parameter simulation	[60]	30.76
5	Scheme based on the PS regime	[63]	32.40
6	Scheme based on the GS regime	[61]	39.52
7	Scheme based on the GS and CS regimes	[61]	39.24
8	Scheme with the ''complex signal''	[62]	61.47
9	Scheme ultraresistant to noise	This paper	−10.01

presented in the table. It is seen from the table that the proposed scheme is inefficient at the negative value of the ratio between the energy per bit to the noise power spectral density, while the other scheme under consideration become inefficient at the positive value of this ratio. Thus, a majority of the known schemes are inefficient when a communications channel is distorted by noises whose powers are less than the power of a transmitted signal. It is clear that the values of such characteristics can vary from one scheme to another. In this respect, the characteristics of schemes based on switching of chaotic regimes and modulation of control parameters are the best among schemes 1–8 ($E_b/N_0 = 30.76$ dB for schemes 2 and 4). However, the positive value of the ratio between the energy per bit and the noise power spectral density indicates the restricted stability under the action of noise and its destructive influence on data transmission.

Scheme 9 proposed herein demonstrates a high level of immunity to noises existing in the communications channel. In addition, its noise source produces larger distortions of a transmitted signal that impede information message decoding by unauthorized users. In this case, noise plays a constructive role, improving the data transmission confidentiality. In other cases, its influence is destructive.

It should be emphasized that changes in the control parameters, the equations of oscillators, and the noise signal characteristics can lead to a change in the quantitative values of the ratio between the energy per bit and the noise power spectral density. However, the order and ratio of these quantities will remain approximately constant. In particular, the similar results were obtained for oscillators proposed by Chua et al. [64] and Rulkov et al. [49] (investigated in Section 3), which were used in transmitting and receiving devices, and different distributions of a noise signal.

CONCLUSIONS

In this study, for the first time, the noise influence on the onset of generalized synchronization in dissipatively coupled chaotic systems with slightly mismatched parameters has been investigated theoretically, numerically, and experimentally. It has been shown that the noise intensity barely affects the threshold of the onset of the synchronous regime for any type of the system and an arbitrary distribution of a random quantity. The results of theoretical considerations were confirmed by numerical simulation data and/or experimental investigations of unidirectionally coupled flow systems and discrete maps. It should be emphasized that the similar results were obtained for spatially-distributed active media that are described by Ginsburg–Landau equations and demonstrate the regime of space-time chaos.

It has been revealed that, in the presence of noise, the behavior of the GS boundary has a characteristic feature that can find practical applications in various fields of science and technology, e.g., in hidden data transmission over communications channels with high noise levels. The hidden data transmission method based on the GS regime is proposed. Since this method is characterized by a sufficiently high level of noise immunity, it is possible to use an additional noise source in the transmitter of a communications channel to enhance the information transmission confi-

dentiality. In addition, this method is easily implemented in practice

ACKNOWLEDGMENTS

This study was supported by the Russian Foundation for Basic Research, project nos. 08-02-00102 and 09-02-92421, and the "Scientific and Scientific-Pedagogical Personal of Innovative Russia" (2009–2013) Federal Target Program.

REFERENCES

1. A. Pikovskii, M. Rozenblyum, and J. Kurths, *Synchronization. A Fundamental Nonlinear Phenomenon* (Tekhnosfera, Moscow, 2003) [in Russian].
2. S. Boccaletti, J. Kurths, G. V. Osipov, et al., Phys. Rep. **366**, 1 (2002).
3. R. Roy, Nature (London) **438**, 298 (2005).
4. H. Jaeger and H. Haas, Science **304** (4), 78 (2008).
5. U. Parlitz, L. O. Chua, L. Kocarev, et al., Int. J. Bifurcation Chaos Appl. Sci. Eng. **2**, 973 (1992).
6. M. K. Cuomo, A. V. Oppenheim, and S. H. Strogatz, IEEE Trans. Circuits Syst. **40**, 626 (1993).
7. Z. L. Yuan and A. J. Shields, Phys. Rev. Lett. **94**, 048901 (2005).
8. G. K. Rohde, J. M. Nichols, and F. Bucholtz, Chaos **18**, 013114 (2008).
9. D. Materassi and M. Basso, Int. J. Bifurcation Chaos Appl. Sci. Eng. **18**, 567 (2008).
10. R. C. Elson, et al., Phys. Rev. Lett. **81**, 5692 (1998).
11. R. Porcher and G. Thomas, Phys. Rev. E **64**, 010902 (2001).
12. L. Glass, Nature (London) **410**, 277 (2001).
13. M. G. Rosenblum, A. S. Pikovsky, and J. Kurths, Fluctuation Noise Lett. **4** (1), L53 (2004).
14. C. M. Ticos, E. Rosa, W. B. Pardo, et al., Phys. Rev. Lett. **85**, 2929 (2000).
15. E. Rosa, C. M. Ticos, W. B. Pardo, et al., Int. J. Bifurcation Chaos Appl. Sci. Eng. **10**, 2551 (2000).
16. A. E. Hramov, A. A. Koronovskii, P. V. Popov, et al., Chaos **15**, 013705 (2005).
17. B. S. Dmitriev, A. Hramov, A. Koronovskii, et al., Phys. Rev. Lett. **102**, 074101 (2009).
18. M. G. Rosenblum, A. S. Pikovsky, and J. Kurths, Phys. Rev. Lett. **76**, 1804 (1996).
19. N. F. Rulkov, M. M. Sushchik, L. S. Tsimring, et al., Phys. Rev. E **51**, 980 (1995).
20. M. G. Rosenblum, A. S. Pikovsky, and J. Kurths, Phys. Rev. Lett. **78**, 4193 (1997).
21. L. M. Pecora and T. L. Carroll, Phys. Rev. Lett. **64**, 821 (1990).
22. S. Fahy and D. R. Hamann, Phys. Rev. Lett. **69**, 761 (1992).
23. A. E. Hramov and A. A. Koronovskii, Chaos **14**, 603 (2004).
24. M. K. Ali, Phys. Rev. E **55**, 4804 (1997).
25. R. Toral, C. R. Mirasso, E. Hernandez-Garsia, O. Piro, Chaos **11**, 665 (2001).
26. V. S. Anishchenko and T. E. Vadivasova, Radiotekh. Elektron. (Moscow) **47**, 133 (2002) [J. Commun. Technol. Electron. **47**, 117 (2002)].
27. C. T. Zhou and J. Kurths, Phys. Rev. Lett. **88**, 230602 (2002).
28. C. T. Zhou, J. Kurths, I. Z. Kiss, et al., Phys. Rev. Lett. **89**, 014101 (2002).
29. S. Kim, W. Lim, A. Jalnine, et al., Phys. Rev. E **67**, 016217 (2003).
30. C. T. Zhou, J. Kurths, E. Allaria, et al., Phys. Rev. E **67**, 015205 (2003).
31. D. S. Goldobin and A. S. Pikovsky, Phys. Rev. E **71**, 045201 (2005).
32. A. E. Hramov, A. A. Koronovskii, and O. I. Moskalenko, Phys. Lett. A **354**, 423 (2006).
33. S. Guan, Y. C. Lai, and C. H. Lai, Phys. Rev. E **73**, 046210 (2006).
34. J. F. Heagy, T. L. Carroll, and L. M. Pecora, Phys. Rev. E **52**, R1253 (1995).
35. D. J. Gauthier and J. C. Bienfang, Phys. Rev. Lett. **77**, 1751 (1996).
36. A. Martian and J. R. Banavar, Phys. Rev. Lett. **72**, 1451 (1994).
37. R. V. Jensen, Phys. Rev. E **58**, R6907 (1998).
38. L. Zhu, A. Raghu, and Y. C. Lai, Phys. Rev. Lett. **86**, 4017 (2001).
39. A. A. Koronovskii, O. I. Moskalenko, P. V. Popov, et al., Izv. Akad. Nauk, Ser. Fiz. **72**, 143 (2008).
40. Koronovskii A.A., Moskalenko O.I., Popov P.V. et al., Pervaya Milya **4** (1), 14 (2008).
41. K. Pyragas, Phys. Rev. E **54**, R4508 (1996).
42. L. M. Pecora, T. L. Carroll, and J. F. Heagy, Phys. Rev. E **52**, 3420 (1995).
43. L. M. Pecora and T. L. Carroll, Phys. Rev. A **44**, 2374 (1991).
44. K. Pyragas, Phys. Rev. E **56**, 5183 (1997).
45. H. D. I. Abarbanel, N. F. Rulkov, and M. M. Sushchik, Phys. Rev. E **53**, 4528 (1996).
46. A. A. Koronovskii, O. I. Moskalenko, and A. E. Khramov, Zh. Tekh. Fiz. **76** (2), 1 (2006) [Tech. Phys. **51**, 143 (2006)].
47. A. E. Hramov and A. A. Koronovskii, Phys. Rev. E **71**, 067201 (2005).
48. N. N. Nikitin, S. V. Pervachev, V. D. Razevig, Avtom. Telemekh. **4**, 133 (1975).
49. N. F. Rulkov, Chaos **6**, 262 (1996).
50. A. E. Hramov, A. A. Koronovskii, M. K. Kurovskaya, et al., Phys. Rev. E **76**, 026206 (2007).
51. A. Uchida, R. McAllister, R. Meucci, et al., Phys. Rev. Lett. **91**, 174101 (2003).
52. Z. Zheng and G. Hu, Phys. Rev. E **62**, 7882 (2000).
53. A. E. Hramov and A. A. Koronovskii, Europhys. Lett. **70**, 169 (2005).
54. A. E. Hramov, A. A. Koronovskii, and O. I. Moskalenko, Europhys. Lett. **72**, 901 (2005).
55. R. Rico-Martinez, K. E. Kreischer, G. Flatgen, et al., Phys. D (Amsterdam) **176**, 1 (2003).

56. B. Sklar, *Digital Communications. Fundamentals and Applications* (Prentice Hall PTK, Upper Saddle River, N. Y., 2001; Vil'yams, Moscow, 2003).

57. E. S. Poberezhskii, *Digital Receiving Devices* (Radio i Svyaz', Moscow, 1987) [in Russian].

58. H. Dedieu, M. P. Kennedy, and M. Hasler, IEEE Trans. Circuits Syst. **40**, 634 (1993).

59. A. S. Dmitriev, A. I. Panas, and S. O. Starkov, Int. J. Bifurcation Chaos Appl. Sci. Eng. **5**), 1249 (1995).

60. T. Yang and L. O. Chua, IEEE Trans. Circuits Syst. **43**, 817 (1996).

61. J. Terry and G. Van Wiggeren, Chaos, Solitons and Fractals **12**, 145 (2001).

62. K. Murali and M. Lakshmanan, Phys. Lett. A **241**, 303 (1998).

63. J. Y. Chen, K. W. Wong, and L. M. Cheng, Chaos **13**, 508 (2003).

64. L. O. Chua, M. Komuro, and T. Matsumoto, IEEE Trans. Circuits Syst. **33**, 1073 (1986).